Available online at www.sciencedirect.com

ScienceDirect

Procedia Structural Integrity 37 (2022) 614–621

Structural Integrity Procedia

www.elsevier.com/locate/procedia

ICSI 2021 The 4th International Conference on Structural Integrity

Security determination in timber structures. Ultimate Load in Critical Sections

Luis Lima[a], Miguel Tortoriello[a]*, Ana Clara Cobas[a], Renso Cichero[a]

[a]*LEMEJ-UNNOBA (Laboratorio de Ensayos de Materiales y Estructuras-Universidad Nacional del Noroeste de Buenos Aires), Sarmiento 1169, Junín 6000, Argentina*

Abstract

To calculate structural security it is necessary to determine its failure mechanism.
In elasto-plastic materials like timber, structural ultimate load arrives when in an n-degree hyperstatic structure the (n+1) plastic hinge is produced.
Consequently, to calculate structural ultimate loads, the modelling of the basic failure mechanism of timber elements is necessary.
In this paper, we propose basic ultimate load models of willow timber elements experimentally determined. They are models of compression, tension and flexural failure mechanisms in elements with a rectangular cross section.
Numerical results will be included.

© 2022 The Authors. Published by Elsevier B.V.
This is an open access article under the CC BY-NC-ND license (https://creativecommons.org/licenses/by-nc-nd/4.0)
Peer-review under responsibility of Pedro Miguel Guimaraes Pires Moreira

Keywords: Structural security; Failure mechanism; Willow timber

1. Introduction

A building must satisfy Serviceability Limit States; they are the conditions to fulfil because acceptable functionality conditions are the reason of the building existence. The construction must anyways have a sufficient security margin also to be acceptable. In this paper we will speak about this second and fundamental condition because if the security margin is not enough the structure can't be accepted for normal use.

* Corresponding author. Tel: +54-9-02477-15586024
E-mail address: miguel.tortoriello@nexo.unnoba.edu.ar

2452-3216 © 2022 The Authors. Published by Elsevier B.V.
This is an open access article under the CC BY-NC-ND license (https://creativecommons.org/licenses/by-nc-nd/4.0)
Peer-review under responsibility of Pedro Miguel Guimaraes Pires Moreira
10.1016/j.prostr.2022.01.130

If we define security as the relation between ultimate load (P_u) and service load (P_s) it is necessary to determinate both values with adequate precision in any kind of structures. (P_s) can be calculated by employing the Theory of Elasticity adapted to timber bodies. But the (P_u) value can't be determined by applying that Theory; it will be necessary to apply an Elasto-Plastic one.

Elasto-Plastic Theories are based on the values of ultimate load capacity of timber bodies under the action of any load or load-system. Consequently, timber structures design implies the concept of mechanical ultimate limit states and their definition means to know the internal configuration of forces at the moment when the body arrive to its ultimate resistant capacity. In other words we must have the possibility to determine the "ultimate resistant mechanisms" under the main kinds of solicitations. The only way to know these mechanisms is to have the support of sufficient experimental results. The aim of this paper is to describe with experimental support the ultimate load capacity of timber willow elements under tension, compression and bending.

In tests results analysis we will suppose that wood is formed by only two elements: linear fibers oriented in a well-defined direction that are immersed in a homogeneous matrix. The matrix can't cut the fibers (Fig. 1).

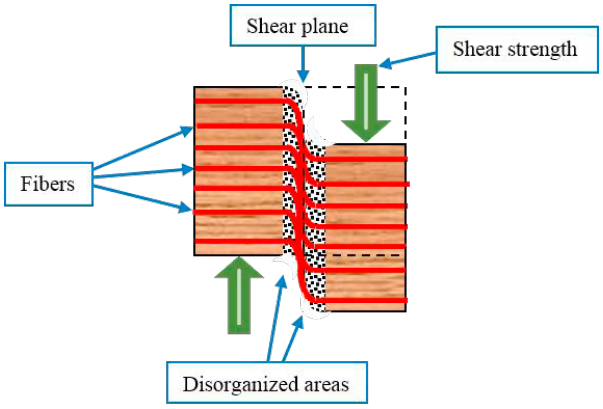

Fig. 1. Cut resistant mechanism.

2. Willow wood characteristics

In Argentina, the Salicaceae (poplars and willows) are used in several industrial applications such as sawn wood, packaging and boards, but mainly in the manufacture of pulp for newsprint. Most of the willow (Willow spp) plantations are established in the Paraná Delta (Buenos Aires and Entre Ríos provinces), where there are excellent ecological and edaphic conditions for the implantation and commercial development of the genus.

Willow is of central importance for forest production in the region, constituting a strength for territorial development. Currently, about 90% of the willow wood produced in the country is used to make paper and particleboard. However, it is also applicable for "solid uses" (sawing and unwinding in the first transformation, and furniture), gaining in recent years a greater interest in this regard. Such is the case, that INTA Concordia is studying willow wood for structural purposes, focused on the construction of social housing.

In recent times, progress has been made, both in knowledge and in dissemination, in the construction of economic wooden houses, highlighting that the economic term is not related to quality, but to a reliable and durable product of a not very high cost. This has motivated the study of species with certain advantages in terms of growth and ease of propagation that were not considered "good" for structural use, as in the case of willow.

There are various studies about the basic density, fiber length and anatomical characteristics of willow wood since these properties influence the quality of the pulp and paper obtained, and it is the industry that mainly consumes this species. Willow wood has basic densities in the order of 350 to 430 kg/m^3 and fiber lengths of 700 to 860 µm −Cobas and Monteoliva (2018); Monteoliva and Cerrillo (2013); Cobas (2013); Villegas et al (2009); Monteoliva et al (2006); Faustino et al (2006); Marlat et al (2002). However, information on the mechanical properties of willow wood is limited (almost nil) in our country. References on these properties have been found in a work presented by Leclercq

(1997) in which he describes willow wood with mean absolute values of resistance to traction, breakage and shear, greater resistance to bending by impact (compared to the Poplar sp.) and an intermediate hardness.

3. Tests specimens

To perform the tests reported we have adopted the following test specimens:

- Axial Tension: prismatic timber parallelepipeds with square section 2.5 cm x 2.5 cm and 21 cm long. To avoid load concentrations in load application zones, the specimens have had their heads enlarged with pieces of wood with the same characteristics and reinforced with hardboard sheets (Fig. 2);
- Axial Compression: three kinds of prismatic timber parallelograms with square section were tested: 1) 2.5 cm x 2.5 cm x 10 cm; 2) 5.0 cm x 5.0 cm x 15 cm; 3) 5.0 cm x 5.0 cm x 25 cm;
- Pure bending (four-forces test): three kinds of prismatic timber parallelograms with square section were tested: 2.5 cm x 2.5 cm x 10[1] cm; 2) 5.0 cm x 5.0 cm x 15 cm; 3) 5.0 cm x 5.0 cm x 25 cm.

Fig. 2. Specimen for tensile test.

4. Tests results

- Axial tension: from 18 specimens tested: $f_{mt,m1} = 55.0$ (MPa)
- Axial compression:
  (5x5x15) cm^3, 15 specimens tested: $f_{mc,m1} = 31.3$ (MPa)
  (5x5x25) cm^3, 7 specimens tested: $f_{mc,m2} = 30.0$ (MPa)
- Pure bending:
  (5x5x60) cm^3, 4 specimens tested: $M_{u,m1} = 96.00$ (kgm)
  (4x4x48) cm^3, 8 specimens tested: $M_{u,m2} = 47.86$ (kgm)
  (2.5x2.5x30) cm^3, 12 specimens tested: $M_{u,m3} = 18.90$ (kgm)

5. Tests results analysis (Ultimate Load Resistant Mechanism)

5.1. Axial tension

5.1.1. Tests description

Applying to the test specimens a uniformly increasing deformation a diagram ($\sigma-\varepsilon$) like the one represented in Fig. 3a is obtained where the corresponding load is also permanently growing from zero (0) to its ultimate value (N_{tu}). When the applied load arrives more or less to 0.5 (N_{tu}) longitudinal cracks appear in the specimen. If external load increases, the number of cracks and their width and length also increases. In failure load proximity, main cracks go from one head to the other (Fig. 3b).

[1] Free length between supports.

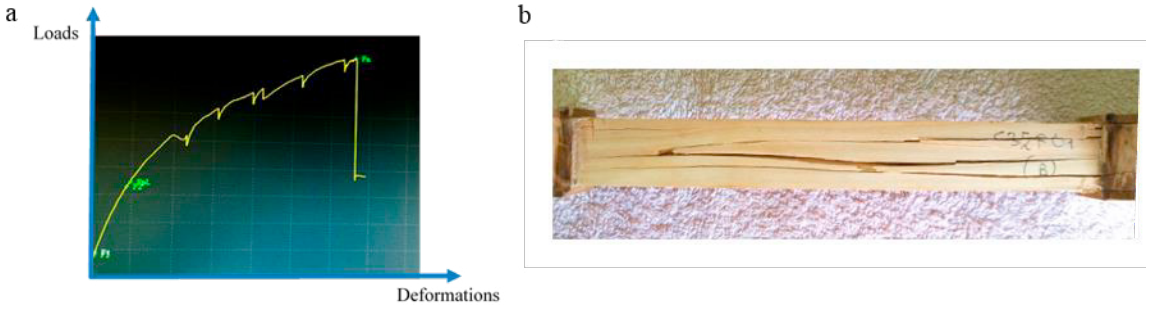

Fig. 3. (a) Loads-deformations diagram; (b) Specimen failure by axial tension.

The specimen is divided longitudinally in a lot of splinters quasi parallel to each other with different normal areas. In any splinter, its normal area changes all along its length. Consequently, normal tensile stress changes in the same way[2] (there is no load transmission between splinters). The failure process begins when the more stressed splinter section fails and consequently the others are surcharged. With a little increase of applied load, another splinter fails, and so on. The specimen collapses when remaining splinters can't resist the applied load.

The approximation to failure load is clear by observing the (σ-ε) diagram, but that is not actually the case. In these conditions the failure is sudden and fragile, and the specimen is divided in two separated pieces.

The origin of lateral stresses which produce longitudinal cracks is the following: test specimens were made with its axis in the direction of wood fibers, but these are not perfectly straight nor perfectly parallel, and when submitted to a tensile stress ─which is only supported by fibers─ the fibers tend to adopt the load direction and transversal stresses appear. When these stresses surpass the wood matrix tensile strength ─that is very low─, cracks appear.

5.1.2. Failure mechanism

For practical applications it is acceptable to suppose a uniform distribution of tensile stresses in sections:

$$f_{tu} = N_{tu} / A_w$$

f_{tu}: ultimate tensile strength
A_w: area normal to wood element axis

Then for structural applications the tensile ultimate limit state may be defined as:

$$N_{tu} = f_{tu} \cdot A_w$$

N_{tu} must be determined experimentally by testing normalized specimens.

5.2. Axial compression

5.2.1. Tests description

When applying to the test specimen a uniformly increasing deformation, an idealized diagram (σ-ε) as the one represented in Fig. 4a is obtained, where it is possible to define three different zones: 1) initially the applied load grows constantly from zero (0) to the maximum value obtained in test process (N_{cu}); 2) then (N_c) values decrease with more or less the same rate; 3) finally specimen deformations grow under an approximately constant load ─in some tests the load increases slightly and in others it decreases slightly─.

[2] It is admissible to suppose that plane sections remain planes in each splinter.

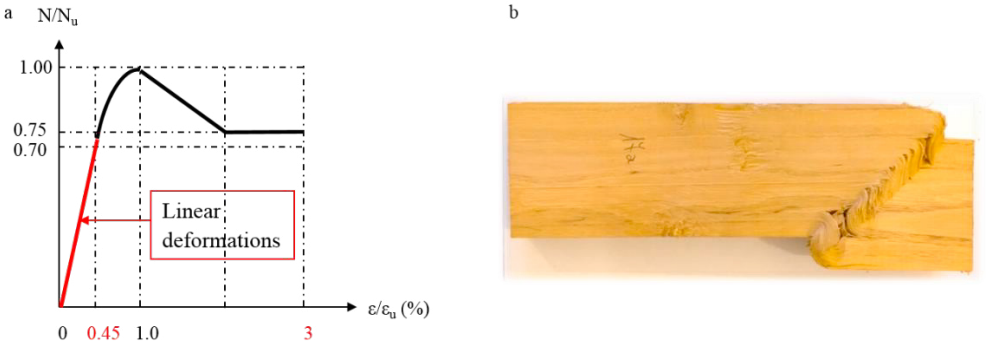

Fig. 4. (a) Idealized diagram in axial compression; (b) Single compression tested specimen.

In the first zone ($0 \leq N_c \leq N_{cu}$) the specimen strength is due to normal compression stresses (σ_c) until ($N_c = N_{cu}$) and ($\varepsilon_c = \varepsilon_{c1}$). Then, the resistant mechanism changes from normal stresses (σ_c) to shear stresses (τ), and a shear fracture plane appears with an angle of (≈50°) from the specimen axis. The tested element is then divided in two pieces that move relatively one to the other. This second zone goes from (ε_1) to ($\varepsilon_{c2} \approx 2 \cdot \varepsilon_{c1}$). Zone 2 is the origin of a shear stresses mechanism which strength is initially only due to matrix shear strength which decreases with the increase of shear strains. In this zone, fibers collaboration is negligible because matrix can't cut them; the applied load decreases from (N_{cu}) to ($N_{cp} \approx 0.75 \cdot N_{cu}$). Finally ─zone 3─ presents shear displacements big enough to produce fibers bending which begin to equilibrate shear forces working in tension (Fig. 4b) and produce the final deformations under constant load.

Failure is completely ductile because the specimen does not lose its integrity, but the initial element axis is broken due to the relative displacement, and secondary effects appear which grow with the increase of the displacements.

5.2.2. Failure mechanism

Under axial load the element has two different compression ultimate limit states. The first is originated by compression stresses and it is valid from ($N_c = 0$) to ($N_c = N_{cu}$). It is represented by the following formula:

$$N_{cu} = f_{cu} \cdot A_w$$

f_{cu}: wood strength in compression

The second compression limit state is a shear one and it is responsible for the element ductility. The plasticization load value (N_p) is:

$$N_p = 0.75 \cdot N_{cu}$$

5.3. Pure bending

The configuration of the tests is show in Fig. 5. All the specimens fail in the central zone [(L/3) ≤ x ≤ (2L/3)] where applied solicitation is pure bending (bending without shear). The tests were performed under controlled deformations normal to support planes.

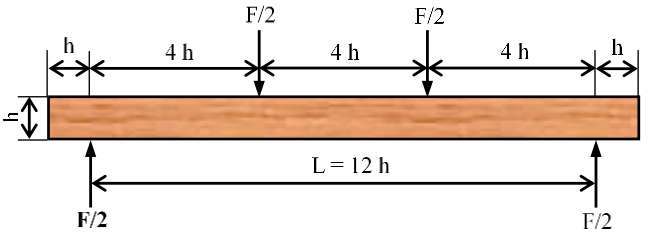

Fig. 5. Pure bending test.

5.3.1. Tests description

The applied loads grow monotonically from zero (0) to failure (M_u) and the obtained diagram (loads-deformations) is show in Fig. 6.

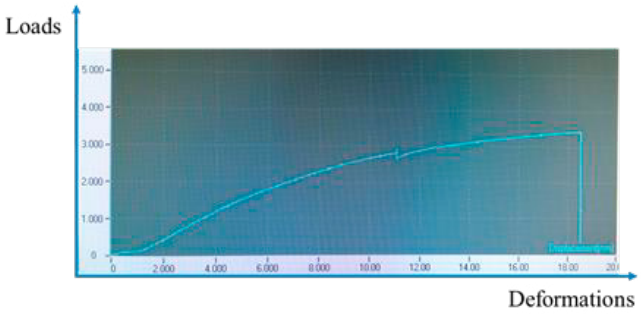

Fig. 6. Loads-deformations diagram.

The first part of this diagram ─more or less until $M = 0.5 \cdot M_u$─ is approximately linear, and it may be analyzed elastically. The second part is curve tending to have a horizontal tangent; the origin of this curvature is the production of horizontal cracks in the lower zone of the beam and near its low face. This scheme is similar to the resistant mechanism in axially tensioned elements. The increase of applied loads produces a progressive plasticization of the stretched zone until all of the fibers arrive to their maximum stresses ($\sigma_{tu} = C_1 \cdot f_{tu}$); then the tensile internal force becomes a constant and consequently also the compression force. If $(M = N \cdot z)$ and $(\Delta M = \Delta N \cdot z + \Delta z \cdot N)$ when (N = constant) the only possibility to resist higher bending solicitations is to increase the (z) value. It is possible to think that the failure process begins when the tensile internal force becomes a constant and in the upper limit of the zone appears an inclined crack or two, one in each direction. The increase of one of these cracks reduces the compressed area and produces the increase of compression stresses. This behavior continues until compression stresses arrive to their ultimate capacity[3] and the specimen fails (Fig. 7).

Fig. 7. Pure bending tested specimen.

[3] As it was show in section 5.2, this value can't be determined in an axial compression test, because in that case the rupture is due to shear and now shear failure is prevented by a flexural resistant mechanism.

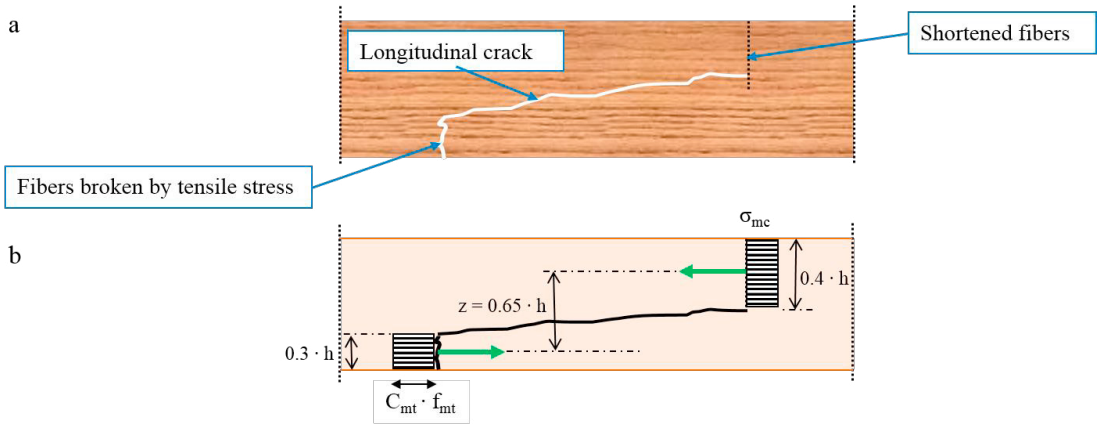

Fig. 8. Pure bending. (a) Rupture scheme; (b) Failure mechanism.

From the rupture scheme shown in Fig. 8a it is possible to establish the failure mechanism in pure bending (Fig. 8b).

5.3.2. Failure mechanism

According to the tests performed (Fig. 8b), the pure bending failure mechanism has the following characteristics:

- Tensile zone height: $0.3 \cdot h$
- Tensile zone area: $0.3 \cdot h \cdot b$
- Compressed zone height: $0.4 \cdot h$
- Compressed zone area: $0.4 \cdot h \cdot b$
- Internal lever arm: $z = 0.65 \cdot h$
- Ultimate tensile stress: $\sigma_{tu} = C_t \cdot f_{tu}$

With the experimental values obtained, it is possible to describe the bending ultimate limit state mechanism which is represented by the following formula:

$$M_u = 0.2 \cdot b \cdot h^2 \cdot (C_t \cdot f_{tu})$$

From these tests we obtain:

$$C_f \approx 1$$

We have assumed that internal compression force is applied at the middle of the compressed area, and any stress diagram that produces a resultant force equal to the tensile force and located in the middle of the compressed zone will be acceptable. The easier solution is to suppose a uniform distribution of compression stresses (f_{cu}), then:

$$f_{cu} = 0.75 \cdot f_{tu}$$

The experimentally obtained ratio between the tensile load limit state and the compression load limit state is 0.55. This difference can be explained if we assume that in pure bending the compression internal force is not transformed to shear resistant force.

6. Conclusions

- The tests performed are sufficient to determine Ultimate Limit States mechanisms, so the proposed ones represent well willow wood failure mechanisms.
- The proposed numerical values are only a basis for discussion, and before any practical applications more numerical experimental data is necessary.
- Four-loads bending tests seem to be the easier way to determine mechanical characteristics of timber elements.
- Results obtained with other kinds of wood of the Salicaceae family show the existence of similar types of Ultimate Resistant Mechanisms.

References

Cobas, A. 2013. Modelos de variación de propiedades del leño juvenil a maduro en Salicáceas y su influencia sobre pulpas quimimecánicas. Tesis de doctorado. La Plata, AR, UNLP. 213 p.

Leclercq, A., 1997. Wood Quality of White Willow. Biotechnology, Agronomy and Society and Environment.

Villegas, S, Area, M. y Marlat, R. 2009. Caracterización de la madera de Salix: Influencia del sitio, clon, edad y altura de muestreo. Investigación Agraria: Sistemas y Recursos Forestales 2009 18(2), 192-203 p